Sādhanā (2022)47:272
https://doi.org/10.1007/s12046-022-02037-4

© Indian Academy of Sciences

Experimental study of scouring downstream of USBR Type I stilling basin aligned with or below the erodible bed

SEYED HAMI HOJJATI, AMIR REZA ZARRATI* and MOJTABA NIKKHAH DEHNAVI

Department of Civil and Environmental Engineering, Amirkabir University of Technology, Tehran, Iran
e-mail: zarrati@aut.ac.ir

MS received 25 July 2021; revised 23 July 2022; accepted 23 October 2022

Abstract. The bed elevation of the stilling basins is most often located below the river bed in order to provide the required tail water depth. Both basins located in alignment with the erodible bed or below it are studied. To this end, the scoured hole dimensions under various circumstances and the sediment transport process within the scour hole were thoroughly examined. Results revealed that the upstream slopes of the dimensionless scour profiles are approximately identical at different times. According to the results, the basin located below the erodible bed was of a greater maximum scour depth and a lower scour depth at the beginning of the erodible bed. Moreover, a simple generalized equation correlating the temporal development of the maximum scour depth and the scour depth at the beginning of the erodible bed at equilibrium time was derived for the USBR Type I basin aligned with or below the erodible bed.

Keywords. Experimental study; scouring; hydraulic jump; USBR Type I stilling basin; scour profile; empirical equation.

1. Introduction

Stilling basins are energy-dissipater hydraulic structures designed to mitigate the destructive energy of the water downstream of overflows and spillways in which the flow energy is dissipated by hydraulic jump [1]. The dimensions of the stilling basins are designed based on the various standards proposed by the USBR[1] [2] and the SAF[2] [3] as some widely used basins in prototype scale.

The erodible bed downstream of the stilling basin may be washed out as a result of the intense turbulence of the flow and the excessive shear stresses. The geometry and extent of the scoured hole are highly affected by the flow characteristics and dimensions of the stilling basin. The results of the previously conducted researches regarding the scouring mechanism portended formation of two roller types within the scoured hole [4, 5]. 1) A backward roller formed through the upstream portion of the hole extending from the location of the maximum scour depth to the beginning of the hole. 2) A forward roller formed at the downstream sector of the hole extending from the location of the maximum scour depth to the end of the hole transporting sediment towards the downstream. The increased water elevation on the scour hole followed by the progression of the scouring phenomenon leads to lower velocities and shear stresses resulting in reduction of the sediment transport capacity of the flow ending in the long run. The sequent depth of the jump, the flow velocity, the length of the basin together with the size and density of bed particles could be regarded as important parameters affecting the dimensions of the scour hole.

From the engineering viewpoint, the upstream slope of the hole and the maximum scour depth will play key roles in design of the stilling basins as extension of scouring in the area and the scoured hole reaching the bottom of the basin may undermine the basin and result in demolition of the structure. Extensive research concerning measurement of scouring profile downstream of hydraulic jumps has been conducted. The equilibrium time of the scouring process so far has been a matter of discordance among researchers as some presume the equilibrium is attained at a particular time [6–8] while others argue that the equilibrium depth may not exist due to the logarithmic temporal progress of the erosion [9]. Researchers namely Farhoudi and Smith (1985) premise that the equilibrium state takes more than 24 hours to be reached called the quasi-equilibrium state [10]. Breusers (1966) [11] proposed an exponential equation for temporal variation of the scour depth downstream an apron of arbitrary length through laboratory experiments reporting identical dimensionless scouring profiles at different times as also declared by Laursen (1952) [12] as well as Breusers (1966) [11]. By investigation of the downstream scour hole for the USBR Type I basin for up to

*For correspondence
Published online: 13 December 2022

[1]United States Bureau of Reclamation.
[2]Saint Anthony Falls.

24 hours, Farhoudi and Smith (1985) observed that the dimensionless scouring profiles were similar at different times [10]. The eventual proposed equation was non-dimensioned with a characteristic length (z^*) and a characteristic time (t^*) where z^* denotes half the height of the spillway while t^* corresponds to the elapsed time until the maximum scour depth equals z^* [10]. Calculation of t^* is associated with complexities hindering estimation of the scour depth using the mentioned equation. Dargahi (2003) [13] proposed a relationship for estimation of the maximum scour depth as a function of the median sediment diameter and the upstream head on the overflow by examination of the scouring downstream and apron of arbitrary length during 8 hours while unlike the observations of Laursen (1952) [12], Breusers (1966) [11] and Farhoudi and Smith (1985) [10] reporting lack of similarity between the obtained scouring profile at any time. In an attempts to investigate the temporal development of the scouring process, Oliveto (2012) proposed an exponential equation for assessment of the maximum scour depth and the pertinent location evaluating the effects of time, sediment diameter, the tail water depth, flow velocity at the end of the apron, sediment density and length of the basin where no similarities between the time-varying scour profiles were detected Oliveto (2012) [14]. The length of the aprons used by Oliveto (2012) [14] was shorter or longer than standard basins and the number of data in each test was limited. Moreover, similarity of scour profiles was studied by various researchers. Among all Altinbelick *et al* (1973) [8] (downstream of the outlet structures), Farhoudi and Khalili (2014) [15] (downstream of the adverse stilling basin) Zahed et al (2011) [16] (downstream of stilling basin with an end sill), and Hassan and Narayanan (1985) [17] (downstream of an apron due to a submerged jet issuing from a sluice gate) can be named. Hojjati and Zarrati [18] numerically studied scouring downstream of USBR basin Type I and using numerical results and existing experimental data presented an equation for the maximum scour depth [18]. In addition, Farhoudi et al (2010) [19] applied the adaptive neuro-fuzzy inference system (ANFIS) to estimate the maximum scour depth downstream of the standard stilling basin with standard error of 0.49 and 0.32 for training and test data, respectively.

It is noteworthy that the results obtained from the previously conducted researches utilizing aprons of various lengths cannot be generalized to the prototype scale as in practice engineers mainly consider standard basins for the design. The Froude number of the performed experiments so far has been limited to values lower than 7. In addition, there are still ambiguities regarding the equilibrium time and the scouring rate in the long run despite the extensive performed research in the relevant field.

In the present study, subsequent to analysis of the scouring mechanism downstream the USBR Type I basin located in alignment with or below the erodible bed, the similarities between the scouring profiles at different times were scrutinized while experimental results for the scouring profiles for a wide range of Froude numbers were also presented. As known, the tail water depth of the basin is determined according to the design flow rate of the spillway. In practice, the bottom elevation of the basin may be located lower than the river bed level (erodible bed) in order to provide the required tail water depth. In the present study, the scouring profile downstream a standard basin located below the erodible bed has also been investigated and compared with the results concerning the basin aligned with the river bed. Finally, using the present and the previous available data an equation was derived for estimating time development of maximum scour depth and the scour depth at the beginning of the erodible bed in the equilibrium state. Due to the fact that in the present study, a wider range of Froude number and a different sediment size was used compared to Farhoudi and Smith (1985) [10] the derived relationship is more general.

2. Experimental set up

The experiments were conducted in a flume 14 m long, 0.3 m wide and 0.65 m high by a recirculating flow mechanism with a flow rate of up to 120 liters per second. The required tail water depth was provided using an adjustable gate at the end of the flume capable of producing various tail water depths. At the beginning of each experiment, the flume was filled very gradually so that the sedimentary bed was saturated. The upstream depth of the flow was controlled by a jet box used to convert the flow inside the pipe to a smooth uniform flow attenuating the shock wave caused by the high-velocity current in transitions to the flume [20, 21]. Application of a jet box facilitated the establishment of uniform flows with a wide range of Froude numbers by changing the flow velocity and depth. In the present study, as mentioned before two sets of experiments were carried out. 1) The standard basin with the same elevation as the erodible bed (SE). 2) The standard basin located below the erodible bed elevation (LE).

The laboratory flume consisting of the jet box, the chute channel, the stilling basin and the downstream erodible bed plus the geometrical properties of the SE and LE basins are presented in Figure 1 in which L_C denotes the length of the chute channel, L_B denotes the length of the basin, L_s represents the length of the erodible bed, z_s corresponds to the height of the erodible bed, z_m is the maximum scour depth, z_0 denotes the scour depth at the beginning of the erodible bed, y_1, y_2 and y_t correspond to the initial depth of the jump, the sequent depth of the jump and the tail water depth respectively. The sequent depth of the jump is calculated using Equation (1) as follows [2]:

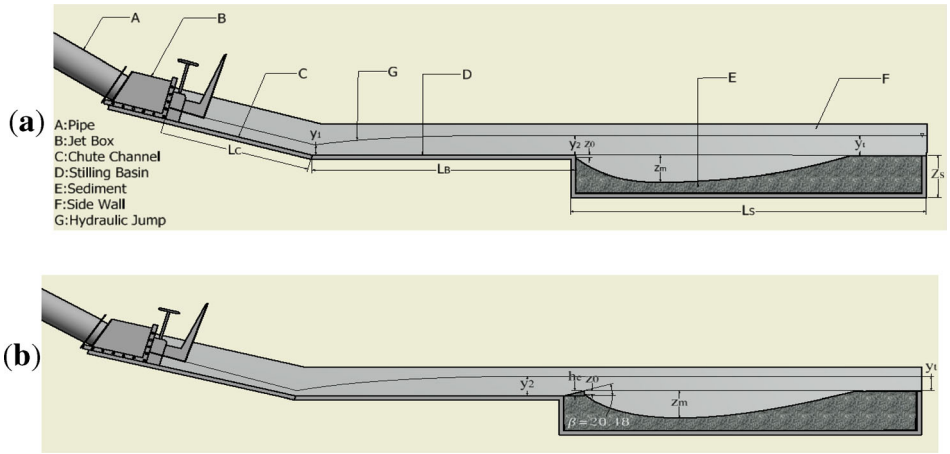

Figure 1. Schematic of the Physical set up for (a) The SE standard basin and (b) The LE standard basin.

$$\frac{y_2}{y_1} = \frac{1}{2}\left(\sqrt{1+8F_r^2} - 1\right) \tag{1}$$

where $F_r = \frac{Q}{By_1\sqrt{gy_1}}$ represents the upstream Froude number, W the width of the channel, Q the flow rate and g the gravitational acceleration. Moreover, the tail water depth is calculated using the equation $y_t = y_2 - h_e$ where h_e denotes the difference in elevation between the bottom of the basin and the erodible bed level.

The length of the examined basin (L_B) in all experiments corresponded to length of the USBR Type I basin. The parameters L_C, L_s, Z_s and W perpetually considered as constants correspond to 130 cm, 300 cm, 36 cm and 30 cm respectively. The length and depth of the erodible bed was selected based on the previous works and trial and error so that the scour hole does not reach the flume bed or the downstream rigid bed. The angel of chute with the horizontal direction was equal to 15 degrees. In the present study, sand particles with median diameter (d_{50}) of 0.54 mm and uniformity coefficient $\sigma = \left(\frac{d_{84}}{d_{16}}\right)^{0.5} = 1.3$ were used. According to Figure 1(b) the bottom of the LE basin was connected to the downstream erodible bed by a constant slope of 1:3 ($\beta = 20.48$) which is usual in executive projects, while the difference in elevation between the erodible bed and the bottom of the basin (h_e) was variant. In the present study three values of 0.12, 0.2 and 0.27 for $\frac{h_e}{y_2}$ were examined. It is worth mentioning that the first 2 cm of the bed downstream the LE basin was implemented horizontally. The sloping part of the LE basin was stabilized using 10 mm gravel. The entire performed experiments regarding the LE and SE basins are listed in Table 1 where $F_d = \frac{V_2}{\sqrt{g'd_{50}}}$ denotes the densimetric Froude number, $g' = \frac{g\Delta\rho}{\rho}$, V_2 is the flow velocity at the end of the stilling basin, ρ and ρ_s are the water and sediment density respectively and $\Delta\rho$ corresponds to the mass density difference between water and the bed material ($\Delta\rho = \rho_s - \rho$). The Froude number of the flow in the conducted experiments was varied by adjustment of the discharge and the height of the jet box gate while the length of the basin for each experiment was designed in accordance to the presented graph in reference [2] for the USBR Type I basin knowing the sequent depth of the jump and the Froude number of the flow. According to the relevant graph, for the range of the Froude number variations in the experiments, the parameter $\frac{L_B}{y_2}$ remains constant and equal to 6.

The experiments were performed by slowly raising the water level inside the channel by y_t prior to the initiation of the test. Subsequent to starting the pump, the flow rate was gradually increased until reaching the desired discharge. In the present study, Exp1 by duration of 1440 min was carried out for long term investigation of the scouring process. The dimensions of the scoured hole were also measured at shorter times and results were extrapolated to see how accurate the long term scour depth can be estimated from shorter time experiments as will be explained in the following sections.

Discharge was measured with a magnetic flow meter of 0.5% accuracy. Flow depth was measured using a Datalogic US30 ultrasonic sensor with an accuracy of 0.5 mm. The scouring profiles were obtained by the aid of the Get Data software measuring the scour depths according to the taken pictures by the Nikon d5300 camera with the f4.5-5.6 18-55 Nikon lens and resolution of 4000 to 6000 (24 megapixel) at different times.

3. Effective parameters

The influential parameters affecting z_m and z_0 are as follows [14]:

Table 1. Experimental tests and the results.

Exp	$\frac{y_2}{d_{50}}$	F_d	F_r	$\frac{h_e}{y_2}$	$\frac{y_2+z_m}{y_2}$ t = 480 min	$\frac{z_0}{y_2}$	$\frac{y_2+z_m}{y_2}$ t = 1440 min
Exp1	487.04	4.07	7.3	–	1.35	0.28	1.43
Exp2	472.22	4.21	6.7	–	1.38	0.27	1.46
Exp3	472.22	4.7	5.55	–	1.43	0.32	1.55
Exp4	472.22	5.09	4.85	–	1.41	0.33	1.49
Exp5	425.93	4.48	5.5	–	1.33	0.18	1.46
Exp6	388.89	4.65	4.8	–	1.29	0.16	1.45
Exp7	472.22	4.21	6.7	0.12	1.44	0.11	1.52
Exp8	472.22	4.7	5.55	0.12	1.47	0.15	1.58
Exp9	472.22	5.09	4.85	0.12	1.46	0.11	1.55
Exp10	472.22	4.21	6.7	0.20	1.47	0.07	1.56
Exp11	472.22	4.7	5.55	0.20	1.51	0.07	1.59
Exp12	472.22	5.09	4.85	0.20	1.48	0.07	1.57
Exp13	472.22	4.21	6.7	0.27	1.54	0.04	1.62
Exp14	472.22	4.7	5.55	0.27	1.63	0.03	1.73
Exp15	472.22	5.09	4.85	0.27	1.59	0.04	1.69

$$z_m, z_0 = f(L_B, \mathrm{V}_2, y_2, \rho, \mu, \rho_s, d_{50}, g, \sigma, t, h_e) \quad (2)$$

where σ is the geometric standard deviation of grain-size distribution, μ is the dynamic viscosity of water and t corresponds to the time of the scouring. Other parameters were defined in previous sections. Using the Buckingham's dimensional analysis method and considering the parameters ρ, y_2 and V_2 as dependent repeating parameters, the previously mentioned relationship takes the following form [14]:

$$\frac{z_m}{y_2}, \frac{z_0}{y_2} = f\left(\frac{L_B}{y_2}, Re, Fr_2, \frac{y_2}{d_{50}}, \frac{\Delta\rho}{\rho}, \sigma, \frac{tV_2}{y_2}, \frac{h_e}{y_2}\right) \quad (3)$$

where $Fr_2 = \frac{V_2}{\sqrt{gy_2}}$ and $Re = \frac{\rho \mathrm{V}_2 y_2}{\mu}$ represent the Froude and Reynolds dimensionless parameters respectively. In the present study, the Reynolds number was consistently greater than 100000. High values of the Reynolds number in this order barely affect the results of the experiments and can be omitted [22–25]. Combination of $\frac{\Delta\rho}{\rho}, \frac{t\mathrm{V}_2}{y_2}, \frac{y_2}{d_{50}}$, and Fr_2 led to the dimensionless temporal parameter $T = \sqrt{\frac{\Delta\rho}{\rho} g d_{50}} \frac{t}{y_2}$ (see reference [14]) while the densimetric Froude number ($F_d = \frac{V_2}{\sqrt{g' d_{50}}}$) was obtained by linkage of the $\frac{\Delta\rho}{\rho}, \frac{y_2}{d_{50}}$ and Fr_2 [14]. The constant dimensionless parameters namely σ and $\frac{\Delta\rho}{\rho}$ can be removed from Equation (2). Moreover, the dimensionless parameters $\frac{z_m}{y_2}$ and $\frac{z_0}{y_2}$ were substituted by $\frac{y_2+z_m}{y_2}$ and $\frac{y_2+z_0}{y_2}$ respectively in order to derive more correlated relationships for calculation of z_m and z_0. Applying the above mentioned alterations, the dimensional parameters affecting the scouring dimensions are as follows:

$$\frac{y_2+z_m}{y_2}, \frac{y_2+z_0}{y_2} = f\left(\frac{L_B}{y_2}, F_d, \frac{y_2}{d_{50}}, T, \frac{h_e}{y_2}\right) \quad (4)$$

4. Scouring downstream of SE stilling basin

The tests Exp1 to Exp6 were carried out for investigation of the scouring process downstream the SE basin for which the Froude number varied in the range of 4.8 to 7.3. In the following section, the temporal development of the scouring process is analyzed following investigation of the scouring mechanism.

4.1 *Scouring mechanism and geometry*

At the beginning of the experiments, the direction of flow near the bed was entirely forward. Thereupon, two distinct flow types were established as the depth of the scour hole was increased over time, the retrogressive flow towards the upstream and the progressive flow towards the downstream. The bed particles transported to the upstream as a result of the retrogressive flow remain in suspension due to the high velocity of the flow carried back towards the downstream. Furthermore, a negligible portion of the particles thrown back in the basin are also carried towards the downstream due to the high flow velocity near the bed. During the early stages of the experiments, the depth of the scouring hole was increased faster than the longitudinal extension and as the scour hole depth increased the upstream slope of the

hole became steeper. Meanwhile reduction of the downstream slope resulted in the further longitudinal development of the scour hole. Further vertical development of the scour hole led to a reduction of the sediment transport in the form of suspended load while the bed load constitutes the principal sediment transport mechanism. According to Figure 2, the bed load within the scour hole was transported in two directions, one part transported through the lowermost depths outflowing downstream of the scour hole while the other part was transported in the opposite direction towards the basin by the turbulent retrogressive flow. The transported sediment towards the basin was again carried towards downstream as suspended load while a part of it fell down into the scour hole. Scrutiny of the entire experiments revealed that the scouring depth variations at the beginning of the erodible bed were trivial after 180 min (Less than 5% variation after 300 min) alluding that after 180 min the sediments transported towards the beginning of the erodible bed were in balance with the eroded sediments thereof leading to insignificant variations thereupon.

The time-varying scouring profiles for Exp1 are presented in Figure 3 as an example according to which the geometry of the scour hole mainly includes three sections; (1) the upstream slope, (2) the bottom of the hole (the lowermost relatively horizontal part) and (3) the downstream slope. As observed in Figure 3, the bottom of the scour hole is geometrically transformed from V-shaped to U-shaped over time with the maximum scour depth moving downstream. The similar tendency was observed in regards with the other experiments as well.

Figure 4 illustrates the temporal variation of the upstream (β_1) and downstream (β_2) average slopes according to which in the preliminary stages of the experiments, the upstream sediments were transported more rapidly due to the retrogressive turbulent currents flowing towards the upstream. By the elapse of time, bed level was lowered and as a result, flow depth increased and velocity decreased. Decrease in velocity caused reduction of sediment transport capacity and scant upstream slope variations within the scour hole after 120 min from the beginning of the experiment. Scrutiny of the downstream slope of the scour hole indicated that in the initial moments of the experiments, the downstream slope of the scoured hole was steepened due to sediment transportation from the upstream reaches of the hole towards the downstream leading to manifestation of the peaks in the curves. Thereupon by continuation of the scouring process the downstream slope of the scour hole was reduced. As the tests progress, the reduction rate of the downstream slope decreased due to the flow depth increment and reduction of the flow velocity.

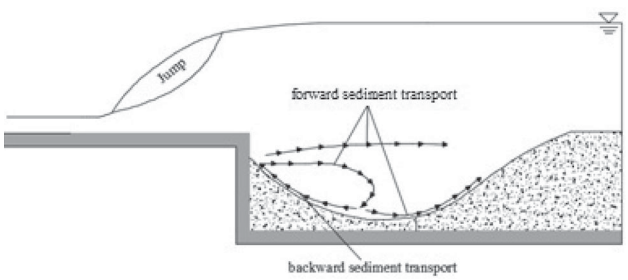

Figure 2. The sediment transport mechanism within the scour hole.

4.2 *Time development of scouring and similarity*

As mentioned previously, various viewpoints on the similarity of the scouring profiles at different times are available some of which put forward by researchers namely Farhoudi and Smith [10] assert the time-independency of the dimensionless scouring profiles downstream SE basin based on z_m while Oliveto [14] and Dargahi [13] argue that no similarities between the scouring profiles at different times were observed. Figure 5 illustrates the geometrical similarities between the scouring profiles regarding Exp1 to Exp6 in which the relevant scouring profiles non-dimensioned based on z_m are presented. According to Figure 5, it is evident that unlike downstream of the scoured hole, the upstream dimensionless profiles at the initial stages of the experiments are almost identical propounding the exclusive geometrical similarity of the upstream profiles. Similar results were obtained non-dimensioning the horizontal axis of the scouring profile based on location of the maximum scouring depth.

The diagram illustrating the dimensionless maximum scour depth (z_m/y_2) versus different dimensionless time (T) regarding time of 8 min to 1440 min for Exp1 are presented in Figure 6. According to this figure it was deduced that a logarithmic curve (in this figure $y = z_m/y_2$ and $x = T$), is capable of accurately estimating the temporal development of the scouring process. According to Figure 6, the increment rate of $\frac{z_m}{y_2}$ is reduced considerably over time as the slope of the graph is asymptotically approaching zero with the elapse of time. Similar diagrams and logarithmic equations were also found for time sections of 8 min to 240 min, 8 min to 480 min, 8 min to 720 min and 8 min to 1080 min.

By extrapolation of the fitted curves within the range of the data at different time sections, the depth of the scouring corresponding to 1440 min was calculated. With respect to the obtained results it was revealed that knowing the maximum scour depths until time sections of 8 min to 240 min, 8 min to 480 min, 8 min to 720 min and 8 min to 1080 min, the maximum scour depth corresponding to 1440 min was calculated by 4.75%, 3.67%, 2.53% and 0.88% of error respectively. In regards with the relatively meager errors concerning the estimation of the maximum scour depth at long term experiment of 1440 min in correlation with the scour depth at time section of 8 min to 480 min, the entire experiments were continued for 480 min and the maximum scour depth at 1440 min was

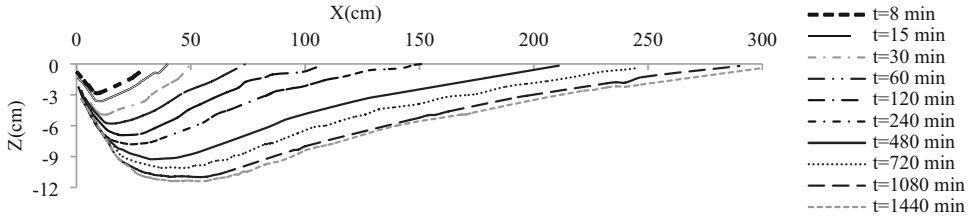

Figure 3. The time-varying scouring profile for Exp1.

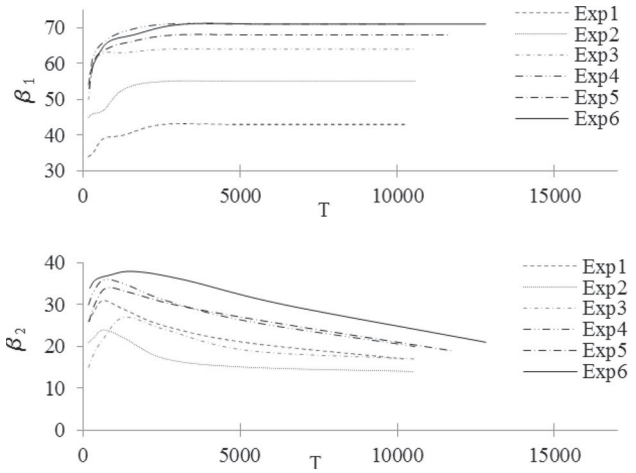

Figure 4. The slope of the scour hole a) the upstream slope b) the downstream slope.

calculated by extrapolation of the fitted curve. In other words, it was revealed that knowing the maximum scour depth 480 min. from the initiation of the experiments, the maximum scour depth at the time section of 1440 min. is estimated fairly accurately. According to Farhoudi and Smith (1985) though scour development reduces considerably after 24 hours but it may increase very gradually in longer times and for that reason they called the scour condition after 24 hours as quasi-equilibrium. Following Farhoudi and Smith (1985) the experiments of the present work were also planned for 24 hours that is the quasi-equilibrium condition (see Figures 3 and 6).

4.3 *Development of an equation for scour depth*

Review of the formerly conducted researches portends impracticability of reaching a general relationship for estimation of the maximum scour depth downstream the SE stilling basin for a wide range of Froude numbers. The relationship proposed by Oliveto (2012) [14] is of a 18% average error while the relationship brought forward by Farhoudi and Smith (1985) [10] is difficult to use. In the present study, attempts have been made in order to present a general simple relationship capable of accurately estimating the maximum scour depth. To this end, the 113 sets of results from the experiments conducted by Farhoudi and Smith (1985) [10] using sand with median diameter varying between 0.15 mm and 0.85 mm with the Froude number and $\frac{L_B}{y_2}$ varying in the range of 3.53–6.63 and 5.57–6.1 respectively, were also utilized of in addition to the obtained results herein. In the 45 experimental data sets of the present study, $\frac{L_B}{y_2}$ is constant and equal to 6 and the flow Froude number is in the range of 4.8 to 7.3. Finally, taking advantage of 158 sets of laboratory experiments 70% of which were considered for training while the remaining 30% were assigned to tests. Based on regression analysis Equation (5) is proposed for the estimation of the maximum scour depth in which $R^2 = 0.82$. The experimental results in regards with estimation of the maximum scour depth for the training and test data are presented in Figure 7. The proposed relationship applies to $\frac{L_B}{y_2}$ varying in the range of 5.57–6.1, F_d varying from 2.06 to 9.17, $\frac{y_2}{d_{50}}$ from 113.18 to 1033.33 and T ranging from 19.07 to 105348.

$$\frac{y_2 + z_m}{y_2} = 1.93 F_d^{0.576} (L_B/y_2)^{-0.153} (y_2/d_{50})^{-0.222} T^{0.055} \quad (5)$$

The mean errors for the training and the test data correspond to 4.99% and 5.63% respectively. Also the standard errors (SE) for the training and the test data correspond to 0.0629 and 0.0682 respectively. The standard error is obtained from Equation (6):

$$SE = \frac{\sqrt{\frac{1}{n}\left(\sum_{i=1}^{n}\left[\left(\frac{y_2+z_m}{y_2}\right)_O - \left(\frac{y_2+z_m}{y_2}\right)_C\right]^2\right)}}{\left(\frac{y_2+z_m}{y_2}\right)_m} \quad (6)$$

where n is the number of observations for scour depth, $\left(\frac{y_2+z_m}{y_2}\right)_m$ is the mean value of parameter $\frac{y_2+z_m}{y_2}$ from the computational data. According to Figure 7, the proposed relationship is of a satisfactory accuracy in calculation of the $\frac{y_2+z_m}{y_2}$. Therefore, the time–varying maximum scour depth is appropriately estimated using Equation (5).

A vertical wall inside the erodible bed is needed at the end of the basin to prevent the basin to be undermined by the extension of the scour hole which can be called terminal cut-off. The height of the terminal cut-off is typically

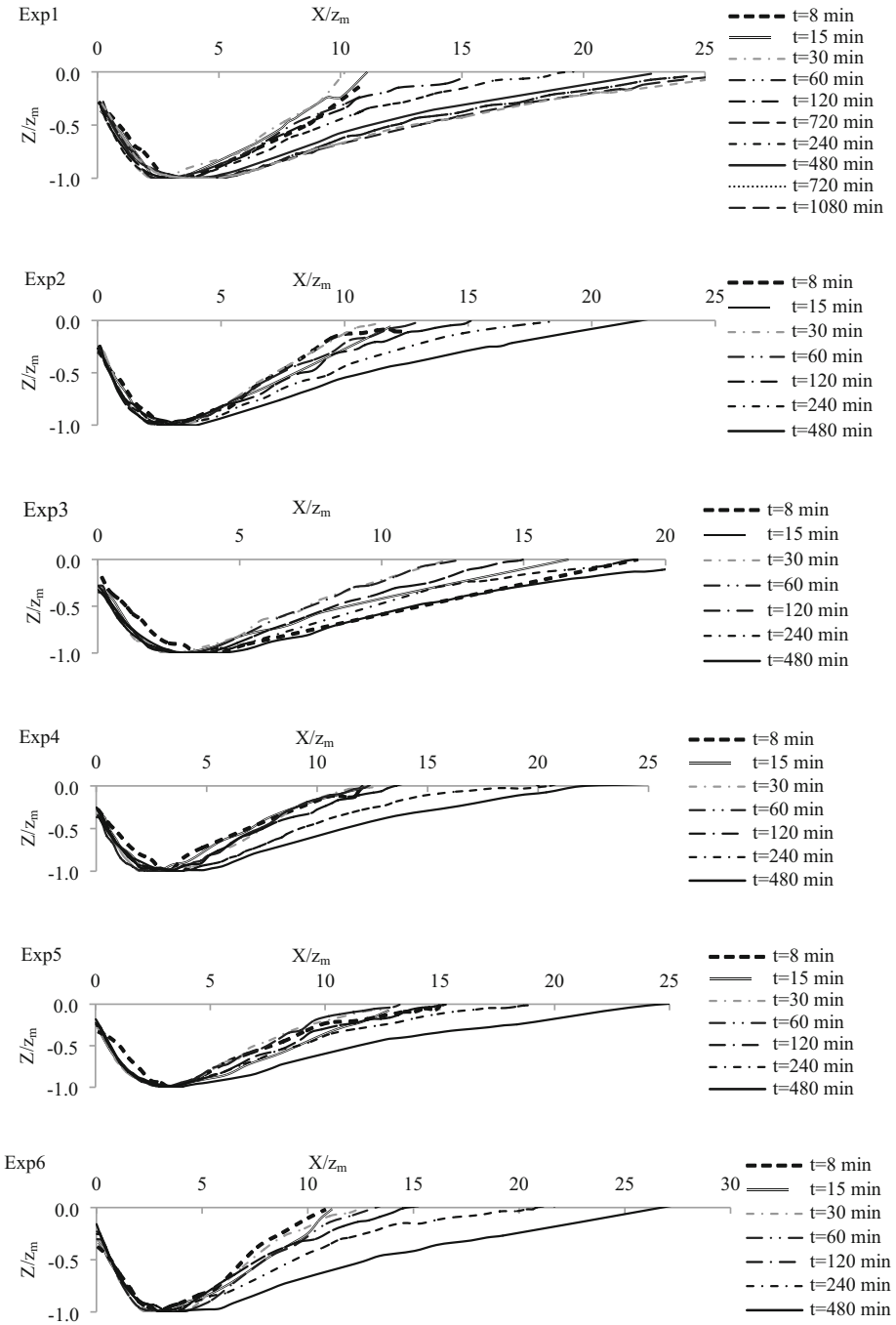

Figure 5. Non-dimensioned scour profile for different times and experiments.

determined based on the z_0 parameter. Therefore, calculation of z_0 is of great importance. In the present study, the results from the 6 sets of conducted experiments on the SE basin together with the results of the 12 sets of tests obtained by Farhoudi and Smith [10] were taken advantage of in order to attain a relationship for calculation of z_0 as no relationship for calculation of z_0 has been presented in the literature so far. Finally, Equation (6) was derived for calculation z_0 under equilibrium conditions to be incorporated in Equation (5). According to Figure 8, the accuracy of Equation (7) is satisfactory with a maximum, mean and standard errors of 4.5%, 1.98% and 0.0224 respectively.

$$\frac{y_2 + z_0}{y_2} = 0.8F_d^{-0.036}(L_B/y_2)^{0.079}(y_2/d_{50})^{0.04} \qquad (7)$$

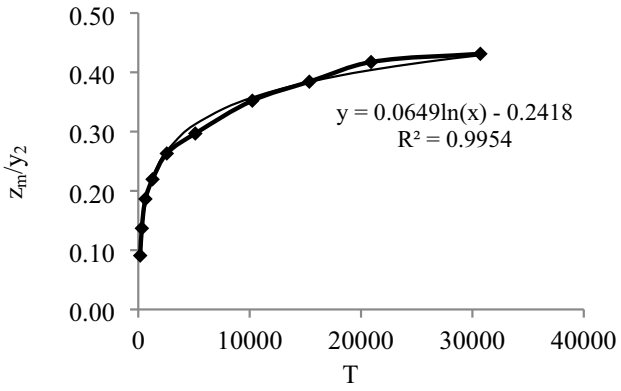

Figure 6. The dimensionless maximum scour depth $\frac{z_m}{y_2}$ versus dimensionless time (T) for Exp1 for test time of 8 hour.

5. Scouring downstream of LE stilling basins

The experiments Exp7 to Exp15 were conducted for investigation of the scouring process downstream the LE basin with the Froude number upstream of the jump varying from 4.85 to 6.7. In accordance to the range of the Froude number and the tailwater depth, the length of the LE and SE basins were the same. The values of the z_0 and z_m parameters corresponding to the experimental time of 480 min are presented in Table 1.

Analogous to SE basin, the dimensionless scouring profiles upstream of the scour hole for the LE basin were almost identical at different times. The maximum scour depth values corresponding to 1440 min. are also presented in Table 1 according to the explanations provided in section 4.2. The LE basin was involved with no scouring mechanism alterations while exhibiting two different flow patterns directly affecting the scouring process; The first alteration was resulted from the difference in elevation at the end of the basin leading to transfer of the hydraulic jump towards the upstream due to the exerted force from the inclined bed to the flow as the lower the basin is located, the further the jump is transferred. The same results were observed for the Type II USBR basin which has end sills at the end of the basin [2]. In the present study, the hydraulic jump was approximately transferred towards the upstream by 7.8%, 11.8% and 34.8% of the length of the basin for values of $\frac{h_e}{y_2}$ equal to 0.12, 0.20 and 0.27 respectively. The intensity of the scouring is anticipated to be depreciated as a result of the turbulent reduction particularly at the beginning of the erodible bed compared to the leveled basin. The second observed difference was issued due to the rise of the sedimentary bed while the tailwater depth remained constant leading to reduction of the water depth on the bed and increment of the flow velocity as a consequence with respect to the continuity equation. The intensity of the scouring is expected to be enhanced because of the increased velocity of the flow. Therefore, one phenomenon resulted in decrement of the scouring intensity in the LE basin while the other acted on the contrary. The reciprocal effect of the interactions between the two phenomena on the scouring process is presented in Figure 9 where each of the parts A, B or C correspond to Froude numbers of 6.7, 5.55 and 4.85 respectively and the scouring profiles were illustrated for various elevation differences between the SE and LE basins at 480 min (the datum for the both basins was intended at the beginning of the erodible bed). According to Figure 9, the maximum scour depth and the distance of the relevant location from the basin is directly proportional to $\frac{h_e}{y_2}$ while, z_0 is inversely proportional to the $\frac{h_e}{y_2}$. Moreover, z_0 for the LE basin is of an extremely lower value compared to the SE basin. As subtraction of the z_0 and z_m are directly related to of $\frac{h_e}{y_2}$, occurrence of the

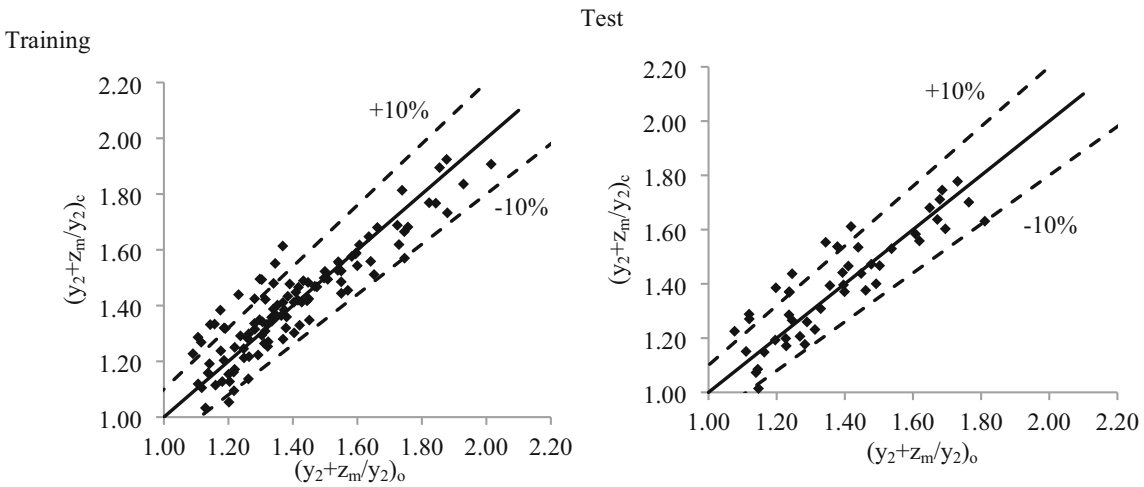

Figure 7. Comparison of the calculated values of the $\frac{y_2+z_m}{y_2}$ (by the "c" index) with the observed values (by the "o" index) thereof using Equation (5).

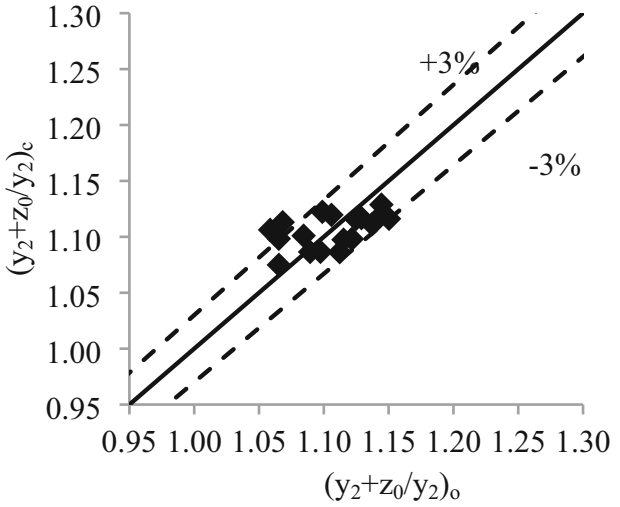

Figure 8. Comparison of the calculated values of the $\frac{y_2+z_0}{y_2}$ (by the "c" index) with the observed values (by the "o" index) thereof using Equation (7).

maximum scour depth further away from the basin slightly affects the upstream slope while the downstream slope of the hole is reduced at higher $\frac{h_s}{y_2}$. The increment percentages of the maximum scour depth (φ_{z_m}) and decrement percentages of scour depth at the beginning of the erodible bed (φ_{z_0}) for the LE basin compared to the SE basin is presented in Table 2 implying that the values of the maximum scour depth for $\frac{h_s}{y_2}$ equal to 0.12, 0.20 and 0.27 was averagely increased by 12.88%, 19.33% and 44.37% respectively compared to the SE basin. In addition, the depth of the scouring at the beginning of the erodible bed for $\frac{h_s}{y_2}$ equal to 0.12, 0.20 and 0.27 was averagely reduced by 53.84%, 72.45% and 84.00% respectively compared to the SE basin. Therefore, it is concluded that the LE basin requires a shorter cut off. It should be noted that in Exp13 to Exp15 the end of the scour hole marginally reached the downstream boundary of the erodible bed and this may have a small effect on the results.

In the present study, the results of 63 laboratory experiments regarding Exp7 to Exp15 at different times for the LE basin revealed that the maximum scour depth in the relevant basin is to be calculated by multiplication of the term $\left(\frac{h_s}{y_2}\right)^{0.027}$ in Equation (5) by maximum and mean errors of 12.04% and 4.88% respectively. According to Figure 10, the accuracy of the proposed equation for estimation of the term $\frac{y_2+z_m}{y_2}$ is corroborated.

The parameter z_0 for the SE and LE basins was approximately invariable after three hours and one hour

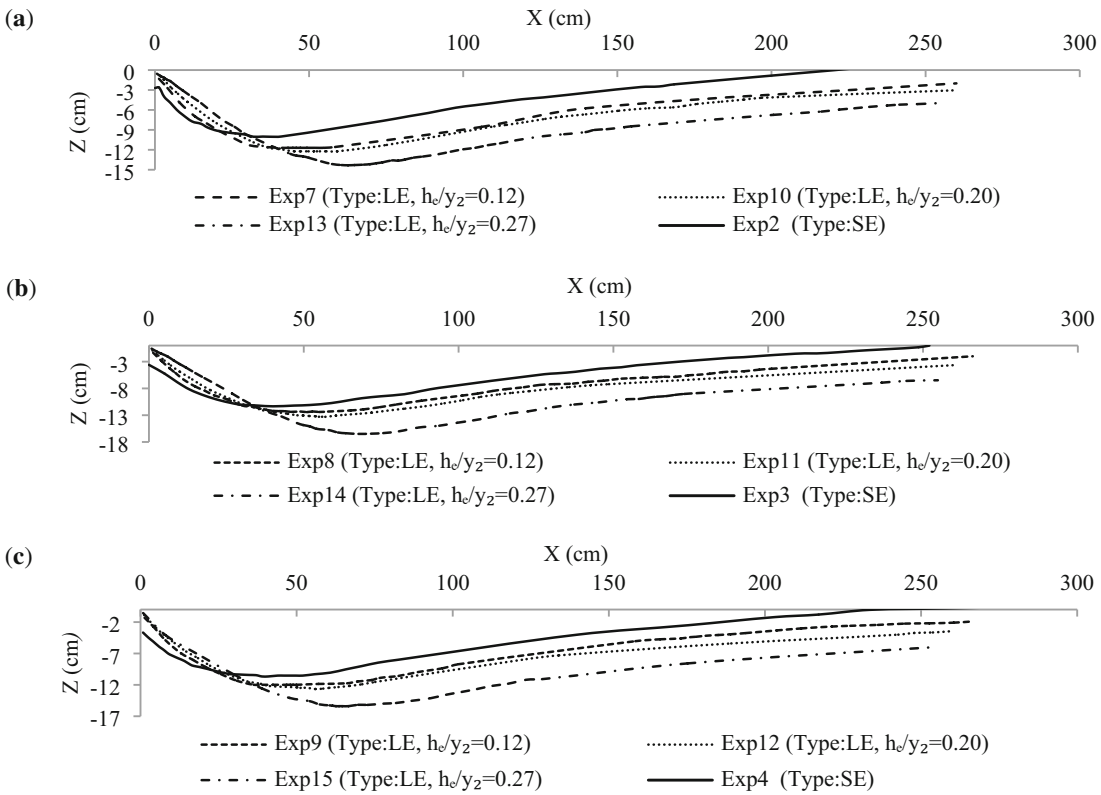

Figure 9. Comparison of the scouring profiles for the LE and SE basins after 480 min. from the beginning of the experiments. (a) For $F_r = 6.7$. (b) For $F_r = 5.55$ and (c) For $F_r = 4.85$.

Table 2. Comparison of z_0 and z_m variation percentage for the LE and SE basins after 480 min. from the beginning of the experiments.

	Exp7	Exp8	Exp9	Exp10	Exp11	Exp12	Exp13	Exp14	Exp15
$\varphi_{z_m}(\%)$	16.65	9.52	12.48	21.93	17.28	18.76	42.77	45.41	44.37
$\varphi_{z_0}(\%)$	51.48	48.33	61.71	67.78	75	74.57	79.63	84.17	84

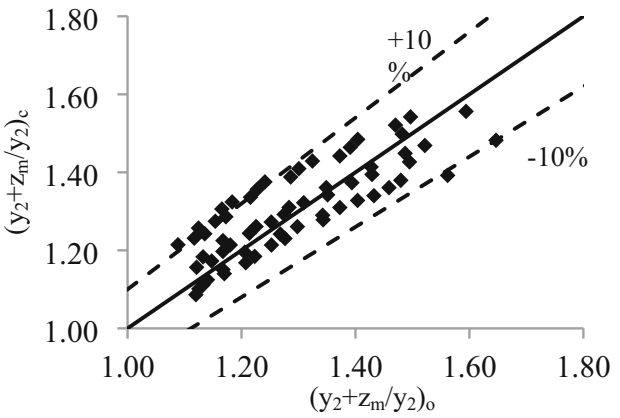

Figure 10. Comparison of the observed values of the $\frac{y_2+z_m}{y_2}$ (The index "o") and the calculated (The index "c") results for the LE basin.

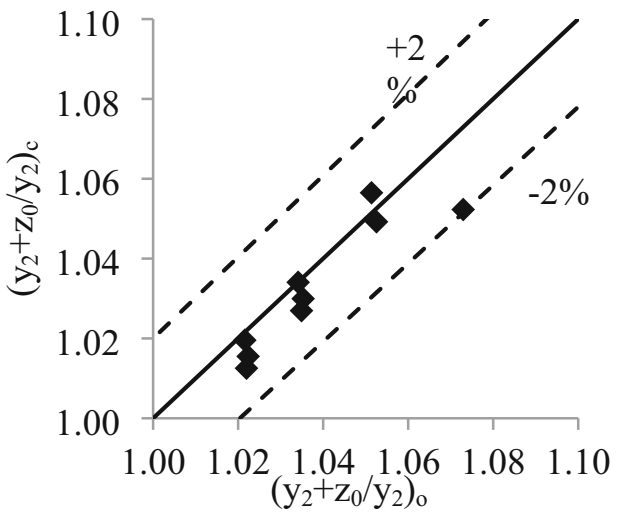

Figure 11. Comparison of the observed values of the $\frac{y_2+z_0}{y_2}$ (The index "o") and the calculated (The index "c") results for the LE basin.

respectively to the uttermost in all experiments (The observed variations were less than 5% beyond the mentioned time sections). As a matter of fact, the term for the LE basin reached equilibrium rather faster than the SE basin. According to the obtained results from the present study, it is inferred that given the results of 9 laboratory experiments for the LE basin, the term z_0 in the relevant basin is to be calculated by changing the constant coefficient of Equation (7) from 0.8 to 0.69 and multiplication of the term $\left(\frac{h_e}{y_2}\right)^{-0.042}$ in Equation (7) by maximum and mean errors of 1.92% and 0.64% respectively. Figure 11 shows the accuracy of the proposed relationship.

6. Conclusions

The present study deal with experimental investigation of the scouring process downstream the standard USBR Type I stilling basin leveled with or below the downstream erodible bed. The profile and dimensions of the scoured hole were analyzed qualitatively and quantitatively via long lasting experiments continued up to 24 hours for a wide range of Froude number and the following conclusions were drawn:

(1) The scour depth at the beginning of the sediment bed and the upstream slope of the scour hole reach equilibrium much faster than the maximum scour depth and downstream slope of the scour hole.
(2) The dimensionless profiles at the upstream sector of the scour hole were almost identical at different times.
(3) A generalized simple relationship for estimation of the time development of the maximum scour depth plus the scour depth at the beginning of the erodible bed at the equilibrium state is proposed based on the obtained results here together with the available experimental data in the literature for stilling basin leveled with the erodible bed.
(4) In the basin below the erodible bed, the hydraulic jump was transferred upstream due to the exertion of the force by the terminal slope of the basin mitigating the intensity of the scouring process while in this case higher velocities increased the dimensions of the scour hole. According to the obtained results, the difference in elevation between the basin and the following erodible bed generally resulted in deeper scour hole. A relationship is also presented for the first time for estimation of the time development of the maximum scour depth and scour depth at the beginning of the sediment bed for the basin located below the erodible bed at the equilibrium time based on the laboratory data of the present study.

(5) It was also concluded that the development of the scouring process at the beginning of the erodible bed is inversely proportional to the difference in elevation between the bottom of the basin and the level of the erodible bed.

List of symbols

W	Channel width
d_{50}	Median grain size
F_d	The densimetric Froude number ($\frac{V_2}{\sqrt{g' d_{50}}}$)
F_r	Upstream Froude number ($\frac{Q}{By_1\sqrt{gy_1}}$)
Fr_2	Downstream Froude number ($\frac{V_2}{\sqrt{gy_2}}$)
g	The gravitational acceleration
g'	$= \frac{g\Delta\rho}{\rho}$
h_e	The difference in elevation between the bottom of the basin and the erodible bed level
L_c	The length of the chute channel
L_B	The length of the basin
L_s	The length of the sediment bed
Q	The flow rate
Re	Reynolds number = $\frac{\rho V_2 y_2}{\mu}$
t	Time of the scouring
t^*	Time required to reach the maximum scour depth equal to z^*
T	The non-dimensional time of scouring ($\sqrt{\frac{\Delta\rho}{\rho} g d_{50}}\frac{t}{y_2}$)
V_2	The velocity of the flow at the end of stilling basin
y_1	The initial depth of the jump
y_2	The sequent water depth of hydraulic jump
y_t	The tail water depth
z^*	Half the spillway height
z_s	The height of the sedimentary bed
z_0	The scour depth at the beginning of the sedimentary bed
z_m	The maximum scour depth at any time
ρ	Density of the fluid
ρ_s	Density of the sediment
$\Delta\rho$	The difference of density between bed material and water ($= \rho_s - \rho$)
β	The slop of LE basin gravel part
β_1	The upstream slop of scoured hole
β_2	The downstream slop of scoured hole
μ	The dynamic viscosity of water
σ	Standard deviation of sediment
φ_{z_m}	The increment percentages of the maximum scour depth for the LE standard basin compared to the SE standard basin
φ_{z_0}	The decrement (φ_{z_0}) percentages of the scour depth at the beginning of the erodible bed for the LE standard basin compared to the SE standard basin

Funding The authors declare that no specific funding was received for this work.

References

[1] Kim Y, Choi G, Park H and Byeon S 2015 Hydraulic jump and energy dissipation with sluice gate. *Water (Switzerland)* 7: 5115–5133. https://doi.org/10.3390/w7095115

[2] Peterka A J (1984) Hydraulic design of stilling basins and energy dissipators. USBR, Denver, CO, A Water Resources Technical Publication, Eng. Monograph 25, 222 pages

[3] Blaisdell F W (1959) The SAF stilling basin: a structure to dissipate the destructive energy in high-velocity flow from spillways. *Agriculture Handbook No 156, US Dept of Agriculture, Agricultural Research Service, Washington, DC*

[4] Ahmad N (1953) Mechanism of erosion below hydraulic works. *Proceedings: Minnesota International Hydraulic Convention*, ASCE, Minneapolis, USA. p. 133–143

[5] Farhoudi J (1979) *Scaling relationships for local scour downstream of stilling basins.* PhD Thesis, University of Southampton , UK, Southampton University

[6] Altinbilek H D (1972) Similarity laws for local scour with special emphasis on vertical circular pipe in oscillatory flow. *Hydraulic Research and Its Impact on the Enviroment*

[7] Altinbilek H D. and Okyay S (1973) Localized scour in a horizontal sand bed under vertical jets. *Proceedings of the 15th IAHR Congress on Research and Practice in the Water Environment, Istanbul, Turkey*, p. 99–106

[8] Altinbilek H Dogan Y (1973) Localized scour at the downstream of outlet structures. *Proceedings of the 11th Congress of Large Dams*, Madrid, Spain. p. 105–121

[9] Rouse H (1940) Criteria for similarity in the transportation of sediment. *Proceedings of the 1st Hydraulic Conference, University of Iowa Studies in Engineering*, State University of Iowa. p. 33–49

[10] Farhoudi J and Smith K V H 1985 Local scour profiles downstream of hydraulic jump. *Journal of Hydraulic Research* 23: 343–358. https://doi.org/10.1080/00221688509499344

[11] Breusers H N C (1966) Conformity and time scale in two-dimensional local scour. *Proc., Symp. on Model and Prototype Conformity, Hydr. Res. Lab*, Poona, India. p. 1–8

[12] Laursen E M (1952) Observations on the nature of scour. Proceedings of 5th Hydrauric Conference., University of Iowa. *Bulletin*, 34: 179–197

[13] Dargahi B 2003 Scour development downstream of a spillway. *Journal of Hydraulic Research* 41: 417–426. https://doi.org/10.1080/00221680309499986

[14] Oliveto G 2012 Local scouring downstream of a spillway with an apron. *Proceedings of the ICE-Water Management* 166: 254–261. https://doi.org/10.1680/wama.11.00101

[15] Farhoudi J and Shayan H K (2014) Investigation on local scour downstream of adverse stilling basins. *Ain Shams Engineering Journal*, Faculty of Engineering, Ain Shams University. 5: 361–375. https://doi.org/10.1016/j.asej.2014.01.002

[16] Zahed E, Farhoudi J and Javan M (2011) Similarity of scour evolution downstream of stilling basin with an end sill. *NEW ASPECTS of FLUID MECHANICS, HEAT TRANSFER and ENVIRONMENT*, 45–49

[17] Hassan N M K N and Narayanan R 1985 Local Scour Downstream of an Apron. *Journal of Hydraulic Engineering* 111: 1371–1385. https://doi.org/10.1061/(ASCE)0733-9429(1985)111:11(1371)

[18] Hojjati S H and Zarrati A R 2021 Numerical study of scouring downstream of a stilling basin. Springer, Environmental Fluid Mechanics, pp 1–18

[19] Farhoudi J, Hosseini S M and Sedghi-Asl M 2010 Application of neuro-fuzzy model to estimate the characteristics of local scour downstream of stilling basins. *Journal of Hydroinformatics* 12: 201–211. https://doi.org/10.2166/hydro.2009.069

[20] Juon R and Hager W H (2000) Flip bucket without and with deflectors. *Journal of Hydraulic Engineering*, American Society of Civil Engineers. 126: 837–845

[21] Schwalt M and Hager W H (1992) Die Strahlbox [The jetbox]. *Schweizer Ingenieur Und Architekt*, 547–549

[22] Haghnazar H and Saneie M (2019) Impacts of pit distance and location on river sand mining management. *Modeling Earth Systems and Environment*, Springer. 5: 1463–1472

[23] Heller V 2011 Scale effects in physical hydraulic engineering models. *Journal of Hydraulic Research* 49: 293–306. https://doi.org/10.1080/00221686.2011.578914

[24] Sangsefidi Y, Mehraein M and Ghodsian M (2018) Experimental study on flow over in-reservoir arced labyrinth weirs. *Flow Measurement and Instrumentation*, Elsevier. 59: 215–224

[25] Sangsefidi Y, Torabi M and Tavakol-Davani H (2020) Discussion on "Laboratory investigation of the discharge coefficient of flow in arced labyrinth weirs with triangular plans" by Monjezi *et al*.(2018). *Flow Measurement and Instrumentation*, 72: 101709